

## Supplementary Information

### Luminescent core-isolated solvent-free liquids as a soft material platform for optical gas sensing

Shinsuke Ishihara,<sup>a,\*†</sup> Avijit Ghosh,<sup>a,b,†</sup> Tatsuya Mori,<sup>a,‡</sup> Mandeep K. Chahal,<sup>a,c</sup> Daniel T Payne,<sup>a,d</sup> Akinori Saeki,<sup>e</sup> Tsuyoshi Hyakutake,<sup>f</sup> Takashi Nakanishi<sup>a,\*</sup>

<sup>a</sup>Research Center for Materials Nanoarchitectonics (MANA), National Institute for Materials Science (NIMS), 1-1 Namiki, Tsukuba, Ibaraki 305-0044, Japan

<sup>b</sup>School of Natural and Applied Science, Department of Forensic Science & Technology, Maulana Abul Kalam Azad University of Technology, Haringhata 741249, West Bengal, India

<sup>c</sup>School of Chemistry and Forensic Science, University of Kent, Canterbury, CT2 7NH, UK

<sup>d</sup>School of Life, Health & Chemical Sciences, The Open University, Milton Keynes, MK7 6AA, UK

<sup>e</sup>Department of Applied Chemistry, Graduate School of Engineering, Osaka University, 2-1 Yamadaoka, Suita, Osaka, 565-0871, Japan

<sup>f</sup>Innovative Materials Resources Research Center, Public Works Research Institute, 1-6 Minamihara, Tsukuba, Ibaraki, 305-8516, Japan.

<sup>†</sup>These authors contributed equally to this work

<sup>‡</sup>Present address: Department of Chemistry, Graduate School of Science and Integrated Research Consortium on Chemical Sciences (IRCCS), Nagoya University, Furo, Chikusa, Nagoya, 464-8602, Japan

\*Correspondence: ISHIHARA.Shinsuke@nims.go.jp, NAKANISHI.Takashi@nims.go.jp

#### Contents

1. Materials
2. General methods
3. Characterizations of **PtPL** and **ZnPL**
4. Photophysical properties of **PtPL**, **PtTPP**, and **PyL**
5. Statistical analysis of sensitivity
6. Microscopic analysis of **PtPL-PTMSP** composites
7. Analysis of residual solvent in a liquid film
8. Coordination property of **ZnPL**
9. References

## 1. Materials

PtCl<sub>2</sub>, benzonitrile, and spectroscopic grade solvents like dichloromethane and toluene were purchased from FUJIFILM Wako Pure Chemical Corp. NMR-solvent CDCl<sub>3</sub>, common reagents for chromatographic purification such as dichloromethane, *n*-hexane, and silica gel 60 N (spherical, neutral) of 40–50  $\mu$ m were supplied by Kanto Chemical. All chemicals and solvents were used as received. Poly(1-trimethylsilyl-1-propyne) (**PTMSP**) was prepared via the polymerization of 1-trimethylsilyl-1-propyne in the presence of TaCl<sub>5</sub> as the catalyst.<sup>S1</sup> Liquid pyrene (**PyL**) was prepared according to our previous report.<sup>S2</sup> Pt(II)-tetraphenyl porphyrin (**PtTPP**) was prepared according to the literature procedure.<sup>S3</sup> Standard gas containing diluted O<sub>2</sub> in N<sub>2</sub> (0.1%, 1%, 10%) were purchased from Suzuki Shokan Co., Ltd.

## 2. General methods

<sup>1</sup>H-NMR and <sup>13</sup>C-NMR spectra were obtained using a JNM-ECS 400 spectrometer (400 MHz, JEOL, Japan), and NMR chemical shifts ( $\delta$ ) are reported in ppm relative to tetramethylsilane (TMS). High resolution electrospray ionization mass spectrometry (ESI-MS) was performed using a Thermo Scientific Q-Exactive Plus with samples dissolved in CH<sub>2</sub>Cl<sub>2</sub>/CH<sub>3</sub>OH. Matrix-assisted laser desorption/ionization time-of-flight mass spectrometry (MALDI-TOF MS) was performed using a Shimadzu MALDI-8030 with dithranol as the matrix. UV-Vis absorption and emission spectra were recorded on a JASCO V-670 spectrophotometer and a JASCO FP-8300 spectrophotometer, respectively. For typical luminescent analyses of solutions, a sample solution (10<sup>-6</sup> M in toluene) was taken into a quartz cuvette (optical length = 1.0 cm) with a rubber septum cap. Two thin needles were inserted into the septum from the top, acting as an inlet and outlet. The solution was slowly bubbled with dry Ar or N<sub>2</sub> for 15 minutes to degas. Although evaporation of toluene was negligible, a few drops of excess toluene may be added beforehand to compensate for evaporation. For luminescent analyses of films, quartz substrates (W × D × H = 25 mm × 10 mm × 1 mm) were used to mount porphyrin films, and placed into a quartz cell (W × D × H = 10 mm × 10 mm × 45 mm) with a rubber septum cap as illustrated in **Figure S1**. Before mounting samples, quartz substrates were sonicated in acetone for 5 min, and then dried with flowing N<sub>2</sub>. Optical microscopy images under polarized and cross-polarized light were obtained using an Olympus BX51 optical microscopy system. Fluorescence microscopy images were obtained using a Leica TCS SP5 confocal laser scanning microscope. Thermogravimetric analysis (TGA) and differential scanning calorimetry (DSC) were performed with a Hitachi TG/DTA 6200 and Hitachi DSC7000X instruments, respectively. The heating rate of TGA and the heating-cooling rate of DSC were both set to 10 K per minute under N<sub>2</sub> gas flow. Phosphorescence lifetime spectroscopies were carried out using a nanosecond laser at 420 nm (10 Hz, 5–8 ns duration, incident photon density = 9.0 × 10<sup>15</sup> photons cm<sup>-2</sup>) from an optical parametric oscillator (OPO, Continuum Inc., Panther) seeded by a Nd:YAG laser (Continuum Inc., Surelite II).<sup>S4</sup> The phosphorescence spectra through an undercut filter (520 nm) at delayed times (1  $\mu$ s gate, 1  $\mu$ s step) were monitored by using an Andor model iStar image-intensifier ICCD camera equipped with a Solar TII model MS2004 monochromator. Absolute quantum yields were determined on a Hamamatsu Photonics Quantaurus C11347.

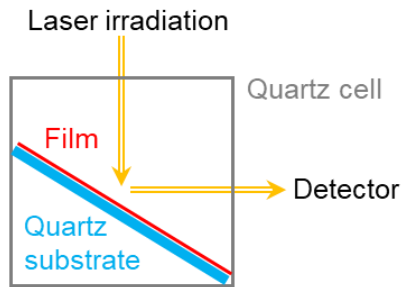


**Figure S1.** Top-view positioning of a sample substrate in a quartz cell.

### 3. Characterizations of PtPL and ZnPL

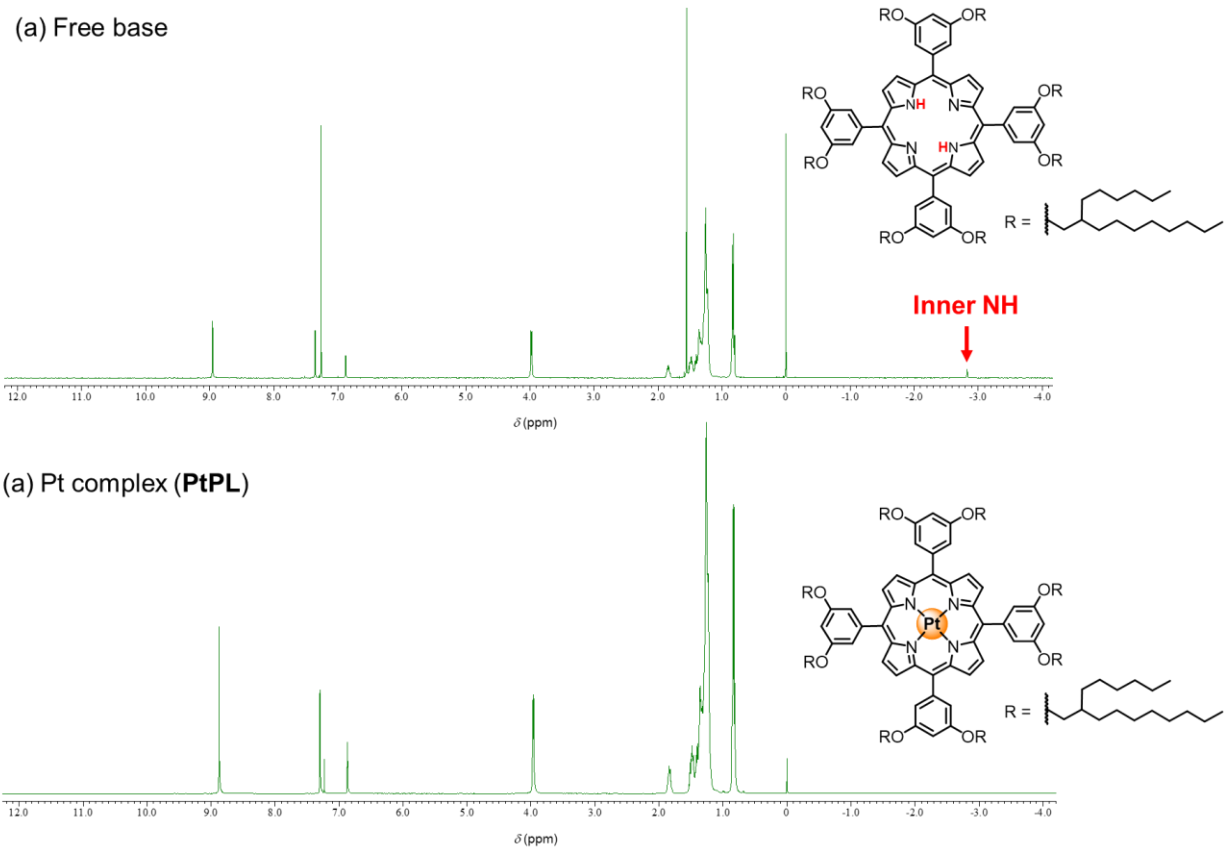


**Figure S2.**  $^1\text{H}$  NMR spectra of the porphyrin liquid (a) before and (b) after insertion of Pt(II) into the core. Note that the inner NH proton signal at  $-2.83$  ppm, characteristic of the free-base porphyrin, disappears after insertion of Pt(II).

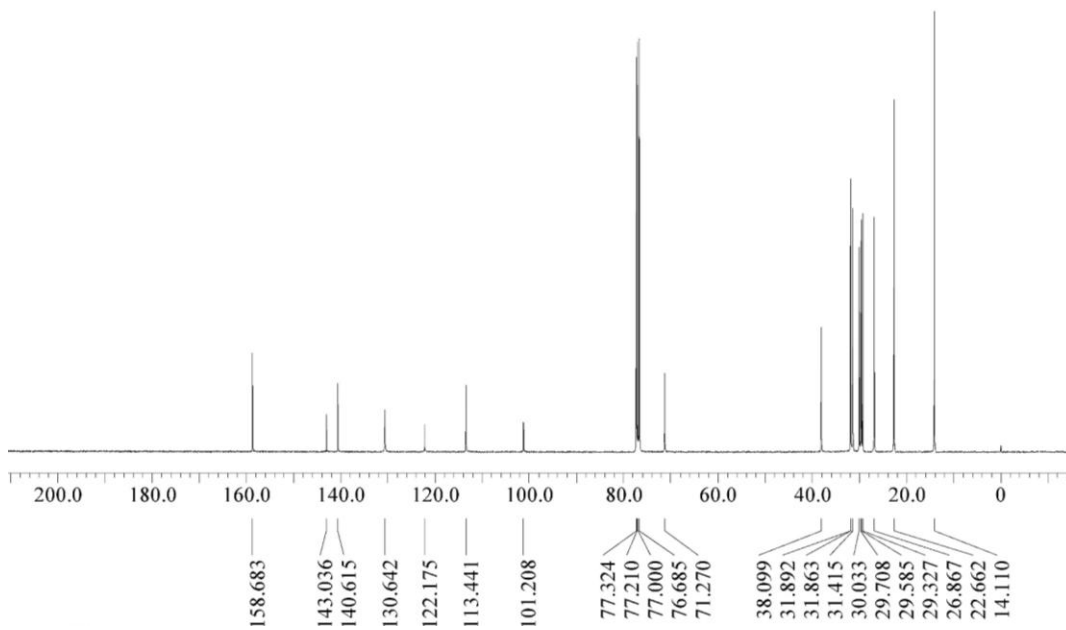


**Figure S3.**  $^{13}\text{C}$  NMR spectrum of PtPL in  $\text{CDCl}_3$ .

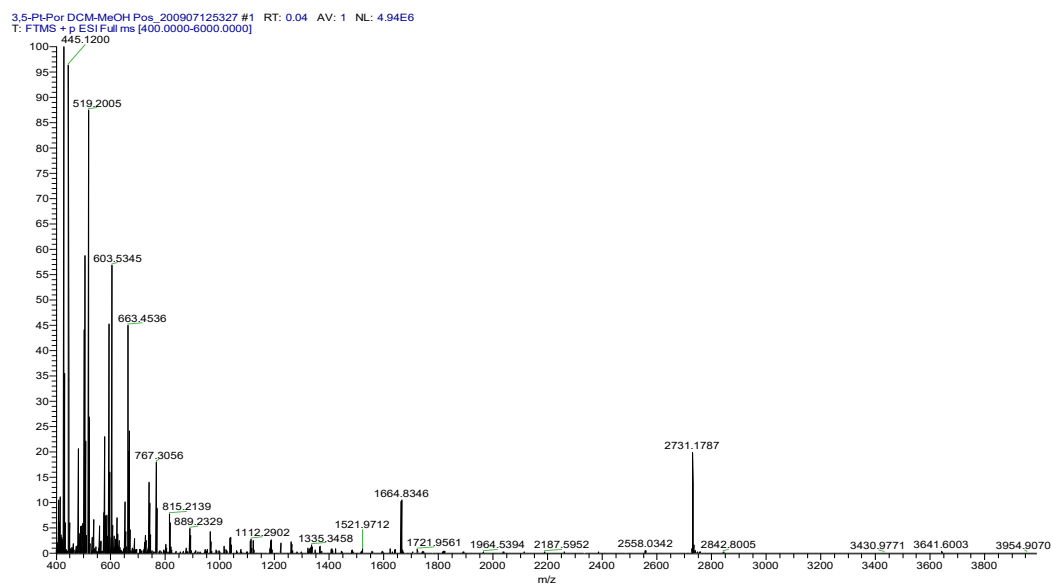


**Figure S4.** HR-ESI-MS spectrum of PtPL in  $\text{CH}_2\text{Cl}_2/\text{CH}_3\text{OH}$  mixture (9:1 in volume).

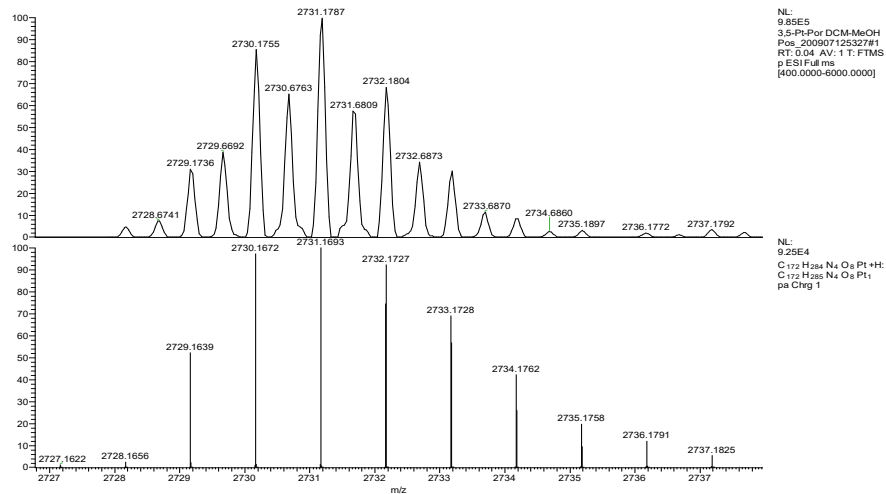


**Figure S5.** Experimental (up) and simulated (down) HR-ESI-MS spectrum of **PtPL** ( $[C_{172}H_{285}O_8N_4^{194}Pt]^{+}$ ). Note that the mass signals appear to contain double-charged dimers ( $z = 2$ ).

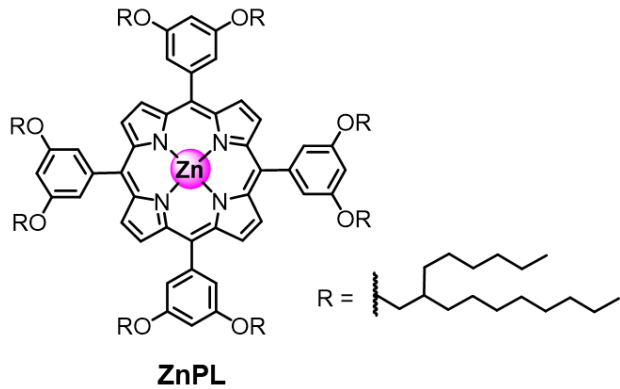


**Figure S6.** Chemical structure of **ZnPL**, an analogue of **PtPL**.

<sup>1</sup>H NMR (400 MHz, CDCl<sub>3</sub>) in ppm: 9.06 (s, 8H, pyrrole  $\beta$ -H), 7.37 (d,  $J = 2.4$  Hz, 8H, Ar-H), 6.88 (t,  $J = 2.4$  Hz, 4H, Ar-H), 3.98 (d,  $J = 6.0$  Hz, 16H, OCH<sub>2</sub>), 1.84 (m, 8H, CH), 1.54-1.20 (m, 192H, CH<sub>2</sub>), 0.82 (m, 48H, CH<sub>3</sub>). <sup>13</sup>C NMR (100 MHz, CDCl<sub>3</sub>) in ppm: 158.60, 150.17, 144.58, 132.11, 121.21, 114.23, 101.17, 71.43, 38.26, 32.02, 32.00, 31.59, 30.18, 29.85, 29.72, 29.46, 27.01, 22.81, 14.23. MALDI-TOF MS (m/z): calculated for  $[C_{172}H_{285}O_8N_4Zn]^{+} = 2599.1264$  m/z, found 2599.7963 m/z.

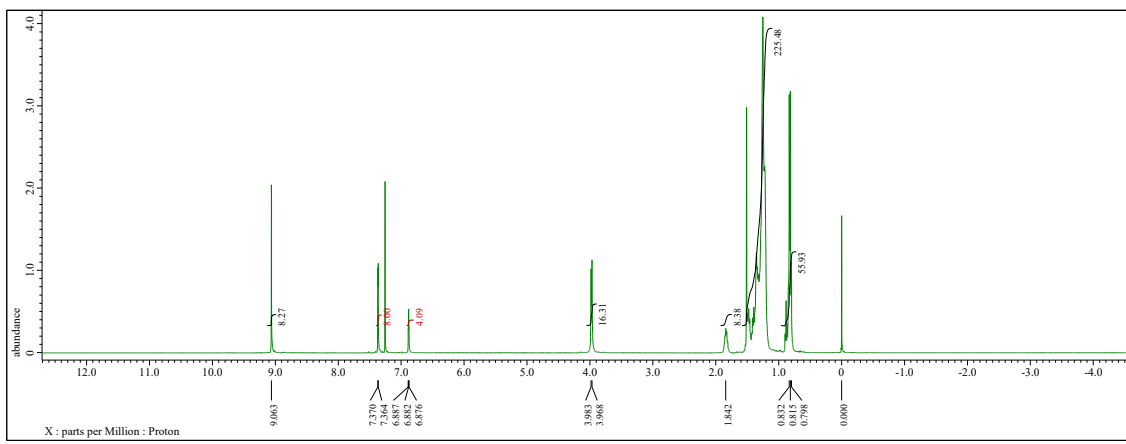


**Figure S7.**  $^1\text{H}$  NMR spectrum of ZnPL in  $\text{CDCl}_3$ .

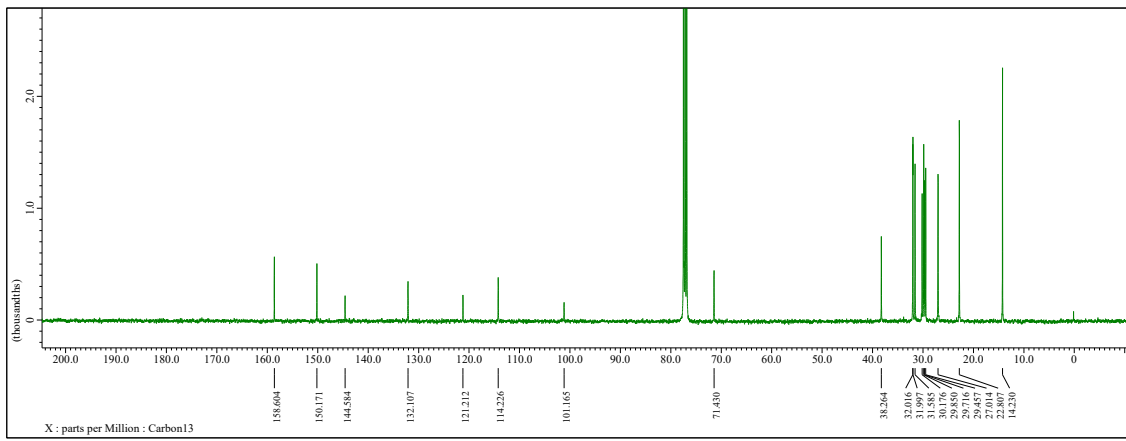


**Figure S8.**  $^{13}\text{C}$  NMR spectrum of ZnPL in  $\text{CDCl}_3$ .

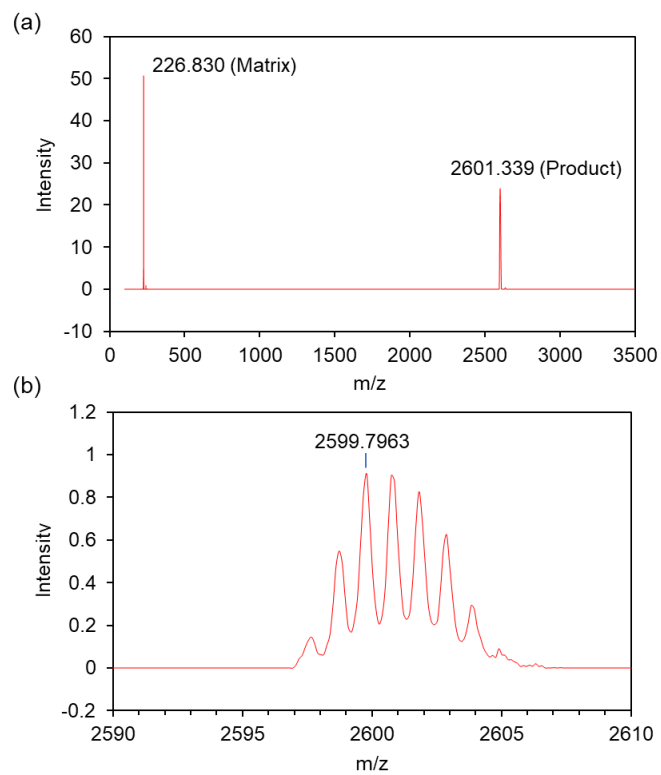


**Figure S9.** MALDI-TOF MS spectra of **ZnP**L measured over (a) a wide m/z range and (b) a narrow m/z range.

#### 4. Photophysical properties of PtPL, PtTPP, and PyL

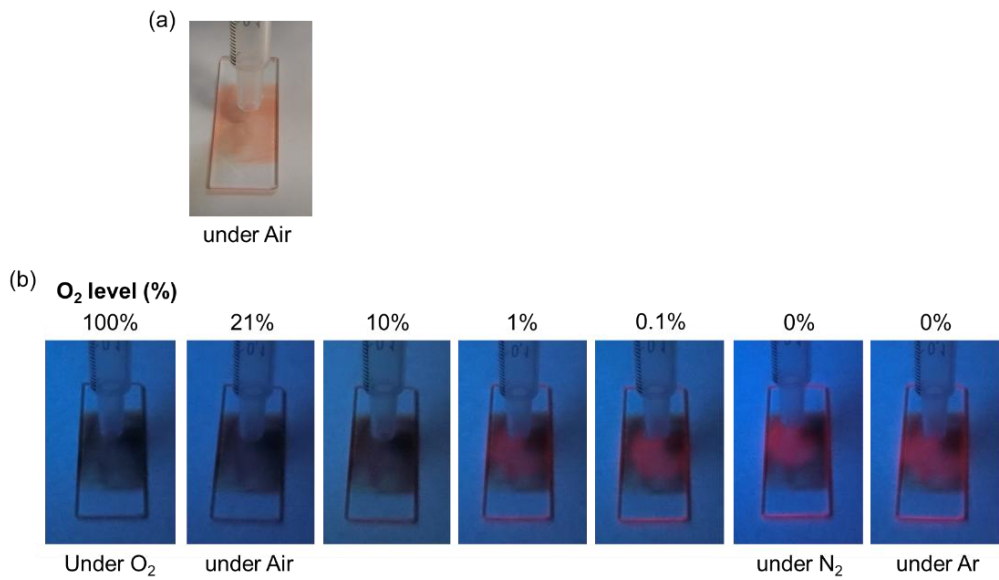


**Figure S10.** (a) Photograph of a neat PtPL film on a glass plate observed under daylight in ambient air. (b) Photographs of the same neat PtPL film observed under UV light (254 nm) with various O<sub>2</sub> levels (0–100%). A high-flow gas (5 L min<sup>-1</sup>) with predefined O<sub>2</sub> levels was blown onto the film in ambient air. All photographs were taken individually using identical camera settings (sensitivity, focus, and exposure time). The results are consistent with those shown in **Figure 3c**, in which the emission intensity decreases exponentially with increasing O<sub>2</sub> levels. Under these conditions, the phosphorescence at 1% O<sub>2</sub> appears slightly weaker to the naked eye than that observed at 0 and 0.1% O<sub>2</sub>. The phosphorescence becomes hardly visible when the O<sub>2</sub> level exceeds 10%.

**Table S1.** Quantum yields of PtPL and PtTPP recorded at room temperature.

Atmosphere	Quantum yield (%)		
	PtPL neat liquid	PtPL in toluene	PtTPP in toluene
Air	1.2	0.6	1.2
Ar	18.2	18.6	14.1

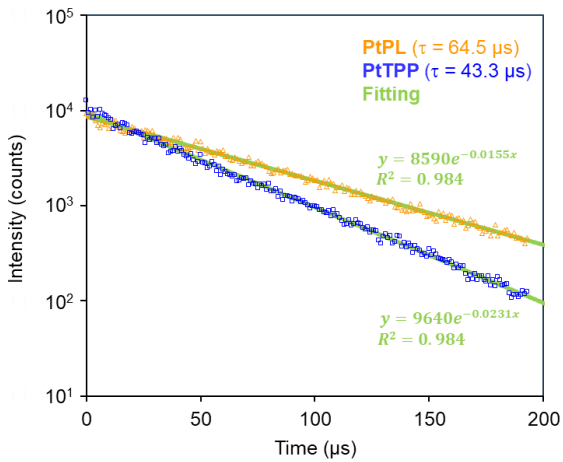


**Figure S11.** Phosphorescence decay profile of **PtPL** and **PtTPP** ( $10^{-6}$  M in toluene,  $\lambda_{\text{ex}} = 420$  nm, ns laser with  $I_0 = 9.0 \times 10^{15}$  photons/cm $^2$ ) after degassing with Ar for 15 min. See **Figure 2** for corresponding absorption and emission spectra. The decay curves were fitted by exponential function. Note that the intensity is plotted on a logarithmic scale and is approaching a plateau when represented on a linear scale.

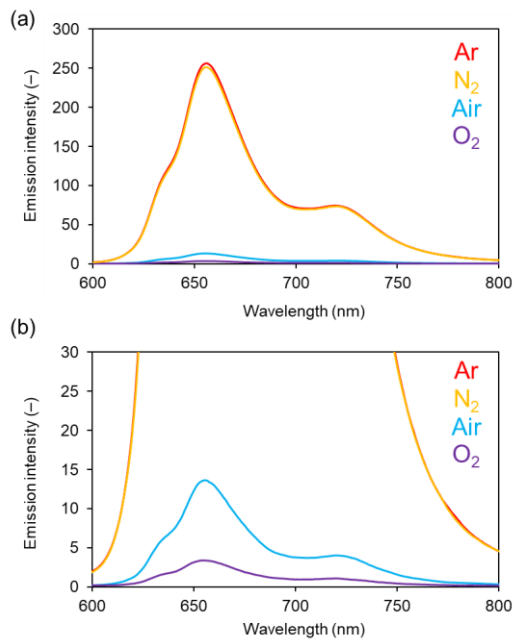


**Figure S12.** Emission spectra of **PtPL** in the neat liquid state measured under Ar, N<sub>2</sub>, air, and O<sub>2</sub> ( $\lambda_{\text{ex}} = 412$  nm): (a) full scale and (b) magnified view.

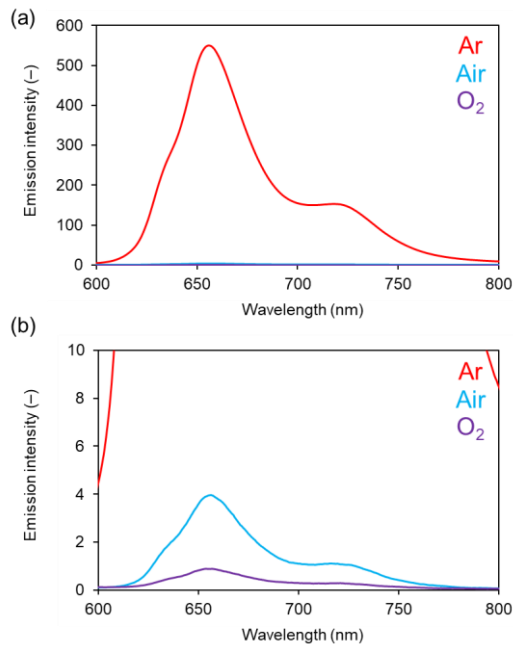


**Figure S13.** Emission spectra of PtPL in toluene (10<sup>-6</sup> M) measured under Ar, air, and O<sub>2</sub> ( $\lambda_{\text{ex}} = 405$  nm): (a) full scale and (b) magnified view.

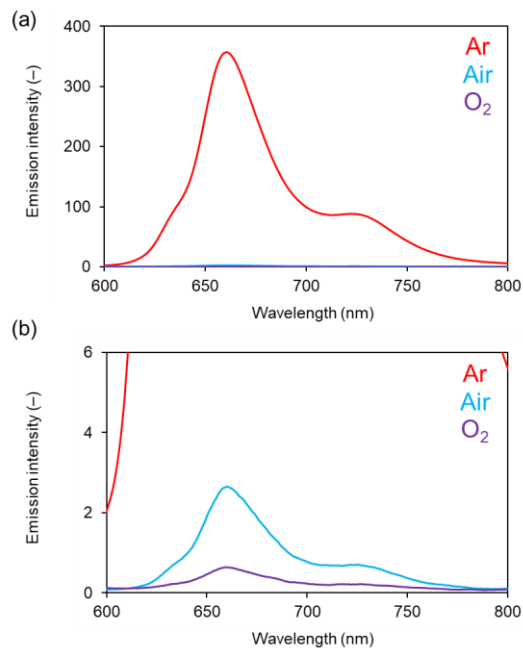


**Figure S14.** Emission spectra of PtTPP in toluene (10<sup>-6</sup> M) measured under Ar, air, and O<sub>2</sub> ( $\lambda_{\text{ex}} = 402$  nm): (a) full scale and (b) magnified view.

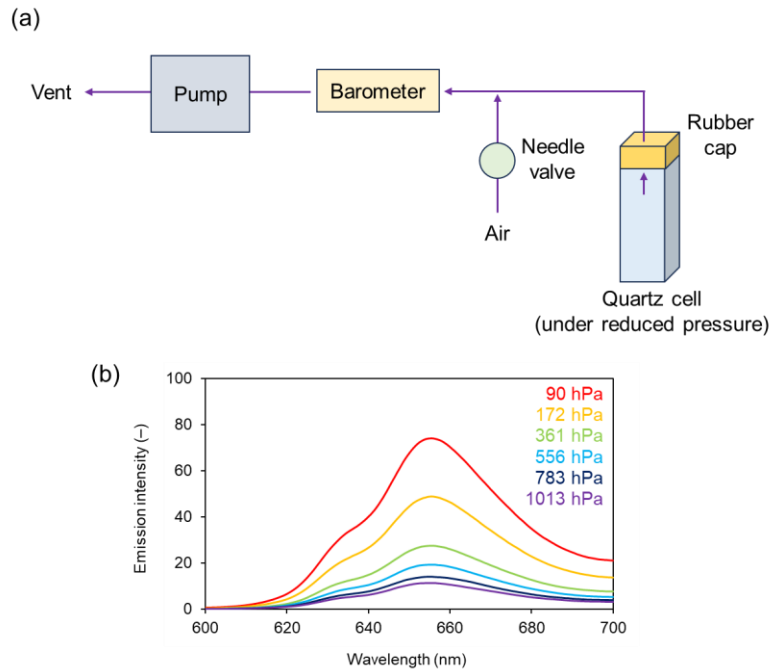


**Figure S15.** (a) Experimental setup for measuring emission spectra under reduced pressure. The air in the quartz cell was partially evacuated without replacement by inert gases (e.g., N<sub>2</sub> or Ar), thereby reducing the partial pressure of O<sub>2</sub>. The air pressure was adjusted using a needle valve, and monitored with a digital barometer (VACUU·VIEW extended, VACUUBRAND). (b) Emission spectra of a neat PtPL film measured under various reduced air pressures.

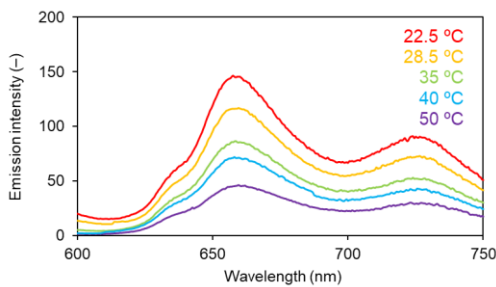


**Figure S16.** Emission spectra of a neat PtPL film measured at various temperatures in air. Temperature was controlled using a cryostat for spectrophotometer (CoolSpek USP-203-B, UNISOKU). Higher temperatures generally increase molecular motion, thereby enhancing non-radiative decay (i.e., quenching of phosphorescence).<sup>55</sup>

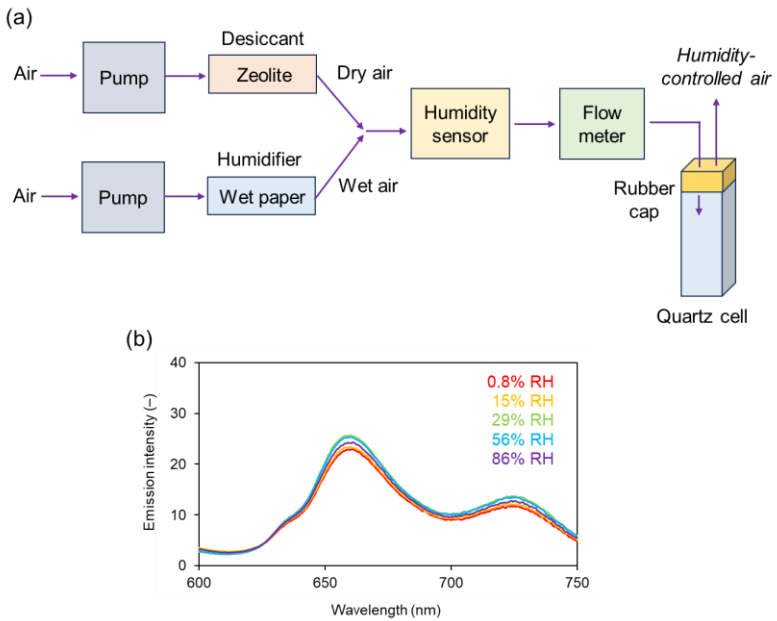


**Figure S17.** (a) Experimental setup for measuring emission spectra under various relative humidities (RH) in air. Ambient air was independently withdrawn using two electrically powered pumps (GSP-400FT, GASTEC) and separately processed to generate dry and humid air by passing through a desiccant (zeolite, synthetic, A-4, shot, 0.50–1.18 mm, Wako Pure Chemical Industries, Ltd.) column and a humidifier (wet paper) column, respectively. These two streams were then mixed at controlled flow rates, with the total flow rate fixed at  $300 \text{ mL min}^{-1}$ . The relative humidity was monitored using a digital humidity sensor (HMI-41, VAISALA). (b) Emission spectra of a neat PtPL film measured under various relative humidity conditions, showing little sensitivity to changes in relative humidity.

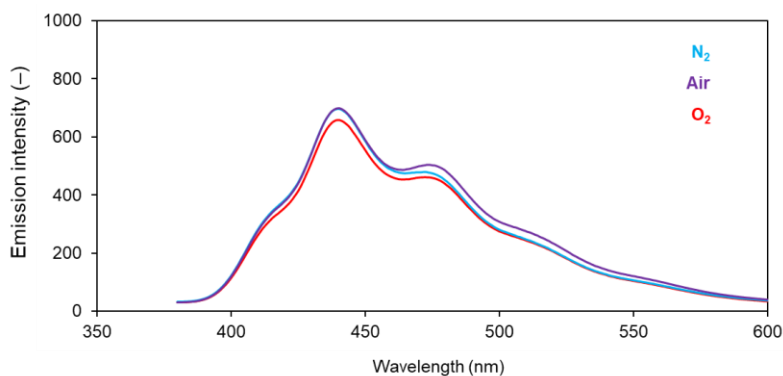


**Figure S18.** Emission spectra of PyL in the neat liquid state ( $\lambda_{\text{ex}} = 360 \text{ nm}$ ) under  $\text{N}_2$ , air, and  $\text{O}_2$ , showing little sensitivity to  $\text{O}_2$  levels.

## 5. Statistical analysis of sensitivity

**Table S2.** O<sub>2</sub> sensitivity ( $I_0/I_{100}$ ) of neat PtPL films ( $n = 6$ ).

Film	1	2	3	4	5	6	Average	$\sigma$
$I_0$	218.2	262.0	196.0	224.7	219.8	285.0		
$I_{100}$	2.85	3.36	2.65	3.00	2.89	3.95		
$I_0/I_{100}$	76.5	77.9	74.1	74.9	75.9	72.2	75.3	1.8

$I_0$ : Emission intensity at 655 nm under N<sub>2</sub> ( $\lambda_{ex} = 412$  nm)

$I_{100}$ : Emission intensity at 655 nm under O<sub>2</sub> ( $\lambda_{ex} = 412$  nm)

$\sigma$ : Standard deviation

**Table S3.** O<sub>2</sub> sensitivity ( $I_0/I_{100}$ ) of mixed liquid films of PtPL+PyL (1:2, by weight) ( $n = 6$ ).

Film	1	2	3	4	5	6	Average	$\sigma$
$I_0$	206.0	175.8	223.7	166.9	278.3	197.4		
$I_{100}$	1.83	1.53	1.95	1.51	2.57	1.67		
$I_0/I_{100}$	112.8	114.8	114.6	110.3	108.3	118.4	113.2	3.3

$I_0$ : Emission intensity at 656 nm under N<sub>2</sub> ( $\lambda_{ex} = 360$  nm)

$I_{100}$ : Emission intensity at 656 nm under O<sub>2</sub> ( $\lambda_{ex} = 360$  nm)

$\sigma$ : Standard deviation

## 6. Microscopic analysis of PtPL-PTMSP composites

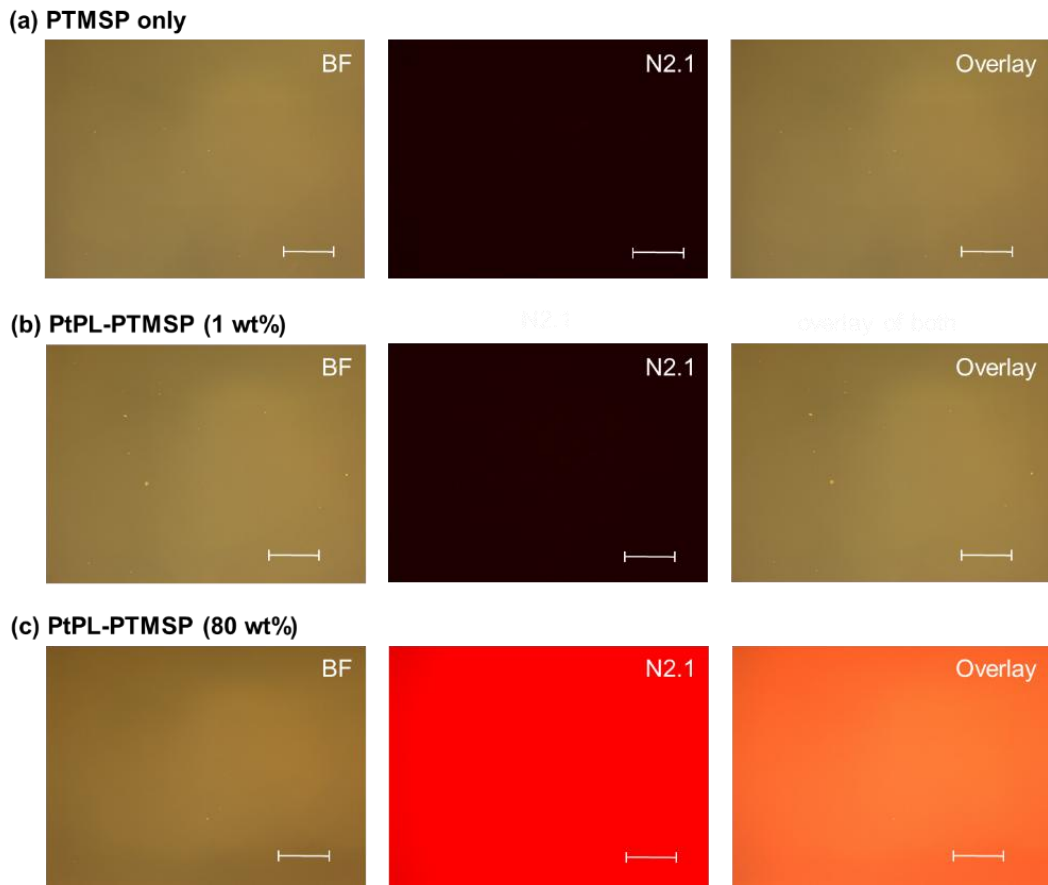


**Figure S19.** Fluorescence microscopy images of **PTMSP** and **PtPL-PTMSP** composite films (1 and 80 wt%). BF and N2.1 indicate bright-field and fluorescence images obtained using the N2.1 (red-channel) filter set, respectively. Scale bar: 200  $\mu$ m. The obtained images show a homogeneous appearance, and no apparent phase separation was observed within the spatial resolution of this technique. These results indicate that the complexes are macroscopically well dispersed. Thus, it is likely that the emergence of multiple emissive states in the Stern–Volmer analysis originates from molecular-level heterogeneity, rather than from microscale or macroscale phase separation.

## 7. Analysis of residual solvent in a liquid film

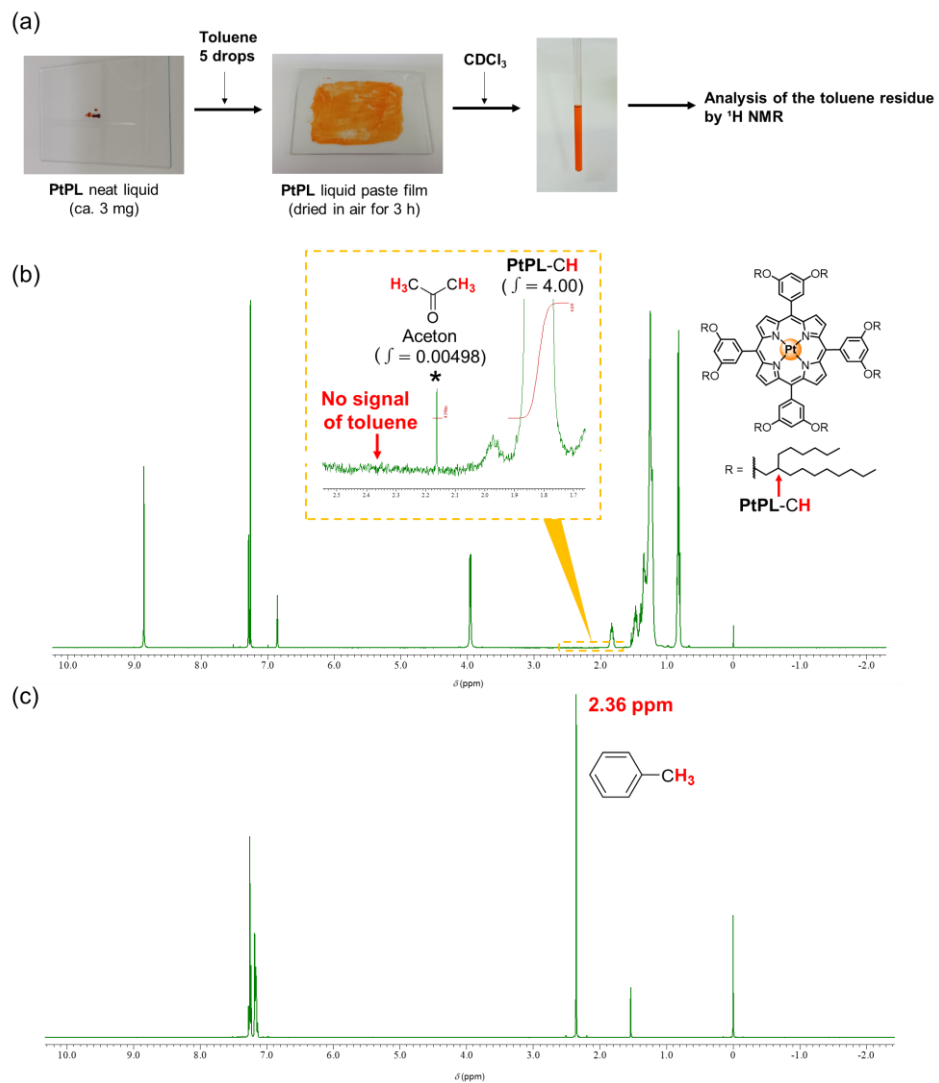


**Figure S20.** (a) Experimental procedure for  $^1\text{H}$  NMR analysis of the toluene residue in a **PtPL** liquid film. The **PtPL** neat liquid (ca. 3 mg) was dissolved in toluene (five drops), spread on a glass plate (5.2 cm  $\times$  7.6 cm) with a spatula, and dried in air for 3 h. The resulting film was then dissolved in  $\text{CDCl}_3$  for  $^1\text{H}$  NMR analysis. (b)  $^1\text{H}$  NMR spectrum of the **PtPL** film in  $\text{CDCl}_3$ , showing the absence of residual toluene. The asterisk (\*) indicates the signal from residual acetone, a common contaminant in chemical laboratories; its amount was estimated by integration to be less than 0.1 mol% relative to **PtPL**. The amount of residual toluene was much smaller than this. (c)  $^1\text{H}$  NMR spectrum of toluene in  $\text{CDCl}_3$ , showing an intense methyl proton signal at 2.36 ppm.

## 8. Coordination property of ZnPL

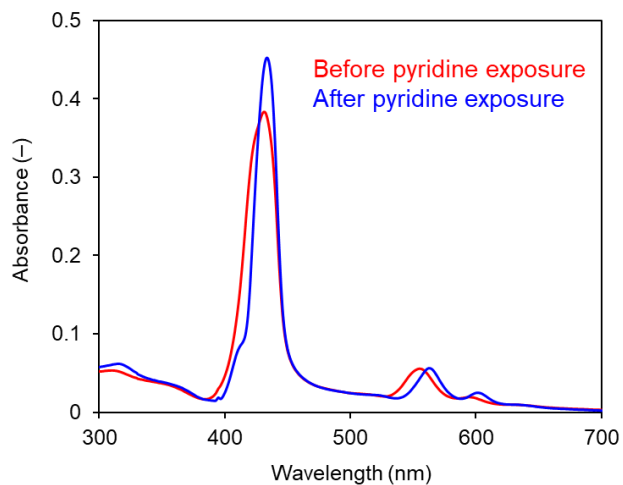
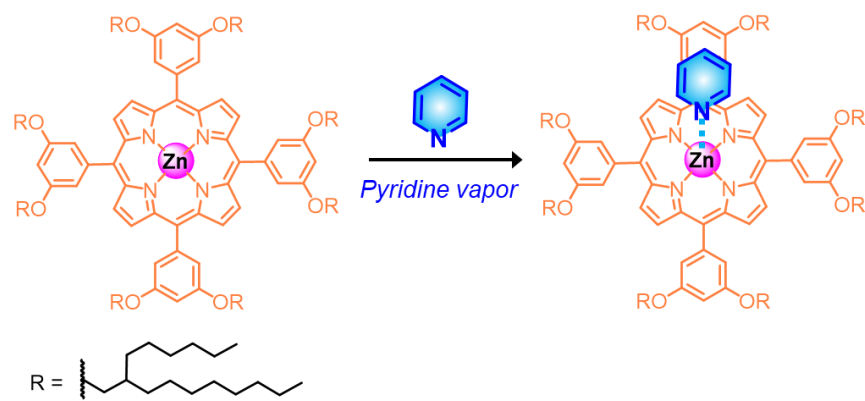


**Figure S21.** (a) Coordination of pyridine vapor by **ZnPL**, an analogue of the **PtPL**. (b) UV-vis absorption spectra of **ZnPL** neat film on quartz plate before and after exposure to pyridine vapor. The red-shift of Soret-band and Q-bands are characteristic to the coordination of ligand molecules on Zn(II) core.

## 9. References

(S1) W. Waskitoaji, T. Hyakutake, J. Kato, M. Watanabe and H. Nishide, Biplanar Visualization of Oxygen Pressure by Sensory Coatings of Luminescent Pt-Porpholactone and -Porphyrin Polymers, *Chem. Lett.*, 2009, **38**, 1164–1165.

(S2) F. Lu, T. Takaya, K. Iwata, I. Kawamura, A. Saeki, M. Ishii, K. Nagura and T. Nakanishi, A Guide to Design Functional Molecular Liquids with Tailorable Properties using Pyrene-Fluorescence as a Probe, *Sci. Rep.*, 2017, **7**, 3416.

(S3) W. Wu, W. Wu, S. Ji, H. Guo, X. Wang and J. Zhao, The Synthesis of 5, 10, 15, 20-Tetraarylporphyrins and their Platinum (II) Complexes as Luminescent Oxygen Sensing Materials, *Dyes Pigm.*, 2011, **89**, 199–211.

(S4) W. Gu, R. Nishikubo and A. Saeki, Coordination of NH<sub>2</sub>- or COOH-Appended Pt-Porphyrins with CsPbBr<sub>3</sub> Perovskite Quantum Dots to Improve a Cascade Process of Two-Photon Absorption and Triplet–Triplet Annihilation, *J. Phys. Chem. C*, 2020, **124**, 14439–14445.

(S5) N. J. Turro, V. Ramamurthy and J. C. Scaiano, Principles of Molecular Photochemistry: An Introduction, University Science Books, Sausalito, CA, 2009.